

**(He<sup>3</sup>, $\alpha$ ) Pickup Reactions in Ni<sup>58</sup> and Ni<sup>60</sup>†**

M. K. BRUSSEL, D. E. RUNDQUIST, AND A. I. YAVIN

*Department of Physics, University of Illinois, Urbana, Illinois*

(Received 7 July 1965)

(He<sup>3</sup>, $\alpha$ ) pickup reactions in Ni<sup>58</sup> and Ni<sup>60</sup> have been studied using 24.5-MeV (He<sup>3</sup>)<sup>++</sup> ions. Several new energy levels in Ni<sup>57</sup> were found. Angular distributions for  $l=1$  neutron transfer were found to be similar to one another, but different from angular distributions for  $l=3$  neutron transfer. A  $j$  dependence of the angular distributions is suggested by the data, and some new spin assignments are proposed.

**I. INTRODUCTION**

IN studies of nuclear structure and nuclear reactions, He<sup>3</sup> has not been as extensively used as protons, deuterons, or alpha particles. Most cyclotrons have not accelerated He<sup>3</sup> ions because of the high cost of He<sup>3</sup>, whereas research with electrostatic accelerators has been limited mostly to low He<sup>3</sup> energies by the nature of these machines. This situation is unfortunate because of the versatility of He<sup>3</sup> when used as a probe for experiments such as elastic and inelastic scattering, charge exchange, pickup, and stripping, all of which start and end with charged particles which are easy to detect and analyze.

Investigations of (He<sup>3</sup>, $\alpha$ ) reactions have been limited to low He<sup>3</sup> energies and light nuclei with few exceptions.<sup>1-4</sup> The (He<sup>3</sup>, $\alpha$ ) reaction is similar to the ( $p,d$ ) and ( $d,t$ ) reactions in that all of these involve the pickup of a neutron. However, accurate information on optical parameters is not as available for He<sup>3</sup> as it is for protons or deuterons. Moreover, the knowledge of the degree of overlap<sup>5</sup> between the internal wave function of the incoming He<sup>3</sup> and outgoing  $\alpha$  is limited. On the other hand, several features of (He<sup>3</sup>, $\alpha$ ) reactions are advantageous or at least complementary to ( $p,d$ ) and ( $d,t$ ) reactions: (a) (He<sup>3</sup>, $\alpha$ ) reactions involve a  $j^\pi=\frac{1}{2}^+$  incoming particle and a  $j^\pi=0^+$  outgoing particle, so that fewer spin channels are open. (b) Whereas ( $p,d$ ) and ( $d,t$ ) reactions enhance low angular-momentum transfers such as  $l=1$ , (He<sup>3</sup>, $\alpha$ ) reactions at medium energies enhance higher angular-momentum transfers such as  $l=3$ .<sup>1,6</sup> (He<sup>3</sup>, $\alpha$ ) experiments therefore complement ( $p,d$ ) and ( $d,t$ ) experiments in that the former can more easily investigate transitions involving high  $l$  which are only weakly excited in the latter. Whenever a mixture such as  $l=1$  and  $l=3$  is observed, it is useful to do both types of experiments. It is unfortunate that very few ( $\alpha$ ,He<sup>3</sup>)

data are available to complement the (He<sup>3</sup>, $\alpha$ ) data the way ( $d,p$ ) and ( $p,d$ ) data complement each other.<sup>7</sup> (c) Sherr, Rost, and Rickey<sup>7</sup> found a  $j$  dependence for  $l=3$  in ( $p,d$ ) reactions at forward angles, using 28-MeV protons. It might be expected that (He<sup>3</sup>, $\alpha$ ) reactions, for which  $l=3$  transitions are enhanced, would be more useful than ( $p,d$ ) reactions in the investigation of such dependence and subsequently for the determination of spins. (d) Although cross sections for (He<sup>3</sup>, $\alpha$ ) reactions are small, it is relatively easy to investigate such reactions because of their large positive  $Q$  values. If the thickness of the particle detector is suitably chosen, no particle identification system is needed for the investigation of a large range of excitations of the residual nuclei corresponding to  $Q>0$ .

We report here on our investigation of the Ni<sup>58</sup>-(He<sup>3</sup>, $\alpha$ )Ni<sup>57</sup> and Ni<sup>60</sup>-(He<sup>3</sup>, $\alpha$ )Ni<sup>59</sup> reactions. All nickel isotopes in their ground states are customarily described to a first approximation as having a closed  $1f_{7/2}$  shell for both neutrons and protons. The picked-up neutron from Ni<sup>58</sup> or Ni<sup>60</sup> is therefore expected to come mostly from the  $1f_{5/2}$  and  $2p$  shells, especially if the residual excitation is low. States of higher excitation may be due to the pickup of a  $f_{7/2}$  neutron, presumably from the core. Whereas Ni<sup>59</sup> has been extensively investigated in both pickup<sup>3,6-9</sup> and stripping<sup>10,11</sup> reactions, Ni<sup>57</sup> has been investigated only via pickup reactions primarily to low-lying states<sup>3,6-8</sup> and only recently to states of higher excitation.<sup>3,9</sup> It should be noted that the pickup of a neutron from Ni<sup>58</sup> is the only way to reach Ni<sup>57</sup> via a nuclear reaction involving light ions.

In this paper we present our experimental data. We observed many distinct groups of alphas with both Ni<sup>58</sup> and Ni<sup>60</sup> targets. These groups correspond to known levels of Ni<sup>57</sup> and Ni<sup>59</sup> as well as to some hitherto unreported levels at higher excitations. We use established  $l$  values to arrive at experimentally determined standard shapes for pure  $l=1$  and  $l=3$  angular distributions ignoring any possible  $j$  dependence. We then employ

† Supported in part by the U. S. Office of Naval Research.

<sup>1</sup> A. G. Blair and H. E. Wegner, Phys. Rev. **127**, 1233 (1962).

<sup>2</sup> C. Glashauser, M. Kondo, M. E. Rickey, and E. Rost, Phys. Letters **14**, 113 (1965).

<sup>3</sup> C. M. Fou and R. W. Zurmuhle, Bull. Am. Phys. Soc. **10**, 496 (1965).

<sup>4</sup> C. Mayer-Börckle, R. H. Siemssen, and L. L. Lee, Jr., Bull. Am. Phys. Soc. **10**, 26 (1965).

<sup>5</sup> M. H. Macfarlane and J. B. French, Rev. Mod. Phys. **32**, 567 (1960).

<sup>6</sup> M. H. Macfarlane, B. J. Raz, J. L. Yntema, and B. Zeidman, Phys. Rev. **127**, 204 (1962).

<sup>7</sup> R. Sherr, E. Rost, and M. E. Rickey, Phys. Rev. Letters **12**, 420 (1964).

<sup>8</sup> J. C. Legg and E. Rost, Phys. Rev. **134**, B752 (1964).

<sup>9</sup> R. Sherr, B. Bayman, E. Rost, M. E. Rickey, and C. G. Hoot, Phys. Rev. **139**, B1272 (1965).

<sup>10</sup> R. H. Fulmer, A. L. McCarthy, and B. L. Cohen, Phys. Rev. **133**, B955 (1964).

<sup>11</sup> L. L. Lee, Jr., and J. P. Schiffer, Phys. Rev. Letters **12**, 108 (1964).

these standardized angular distributions for  $l=1$  and  $l=3$  to infer the angular-momentum transfer for some other transitions. Next, we use known  $j$  values to look for a possible difference between  $j=l+\frac{1}{2}$  and  $j=l-\frac{1}{2}$  angular distributions for each of the  $l$ 's. Such a difference is found and is used to determine other  $j$  values. No distorted-wave analysis has yet been attempted for our data.

## II. EXPERIMENTAL APPARATUS

The He<sup>3</sup> beam used in this experiment was obtained from the University of Illinois isochronous cyclotron.<sup>12</sup> In order to conserve the amount of He<sup>3</sup> used, a 5:1 mixture of He<sup>4</sup> to He<sup>3</sup> was fed into the ion source of the cyclotron. It was found that such a mixture would provide internal cyclotron beam currents of 50–100 μA with little difficulty. With this mixture the amount of He<sup>3</sup> consumed was about 1 cc (STP) per minute.

Approximately 40% of the internal beam was extracted from the cyclotron. An energy of from 12 to 35 MeV could be spanned by suitably adjusting the cyclotron parameters. After extraction, the beam passed through focusing and deflecting elements into the experimental area. The beam entered a 28-in.-diam scattering chamber through two 0.100-in.-diam defining slits placed 16 in. apart. It was subsequently collected in an internal Faraday cup. A solid-state detector was used to monitor the target thickness and beam-intensity distribution during the experiment. In practice the monitor was used to compute the relative cross sections. The energy spread of the beam in the scattering chamber was approximately 100 keV in the present experiment which employed a beam energy of 24.5 MeV. Various beam intensities were used, the maximum being approximately 0.5 μA.

The Ni<sup>58</sup> and Ni<sup>60</sup> targets (purchased from Oak Ridge National Laboratory) used in these measurements had isotopic purities of 99.9% and 99.8% and thicknesses of 0.43 mg/cm<sup>2</sup> and 0.59 mg/cm<sup>2</sup>, respectively. The thicknesses were determined by weight and area measurements, as well as by measurements of the energy loss of alpha particles from a natural source.

Particles emanating from the targets were detected by surface-barrier detectors. Because the Ni<sup>58</sup>(He<sup>3</sup>, α)-Ni<sup>57</sup> and Ni<sup>60</sup>(He<sup>3</sup>, α)-Ni<sup>59</sup> reactions have positive  $Q$  values of about 9 MeV, it was a simple matter to distinguish the α particles from other possible reaction products. A detector thickness just sufficient to stop 35-MeV α particles was employed to this end. The only other  $Q>0$  events, which can produce competing charged particles, result from (He<sup>3</sup>,  $p$ ) reactions. The protons here produced penetrate through the detector, depositing at most 9 MeV. A second detector placed behind the one recording the α-particle events was

occasionally employed as an anticoincidence counter to reject all events for which particles penetrated both detectors. The detectors used were cooled by circulating alcohol through the detector mounting block, the alcohol having been cooled in an alcohol-dry ice mixture. The detector resolution was thereby kept below 40 keV. The over-all energy resolution obtained for the peaks in our data was approximately 120 keV, the difference primarily arising from the beam-energy spread.

The energy of the incident He<sup>3</sup> beam is determined only crudely by the cyclotron operating parameters. To determine this energy more precisely we compared the pulse heights obtained from Po<sup>212</sup>-Bi<sup>212</sup> alphas with the observed pulse heights in the He<sup>3</sup>-induced reactions, specifically the elastic-scattering peaks and the (He<sup>3</sup>, α) ground-state peaks. The electronics employed for the present measurements were conventional. Pulse-height spectra were recorded on a multichannel pulse-height analyzer. Usually 512-channel spectra were taken for any given run.

A troublesome feature which distorted the observed spectra occurred at forward scattering angles, where the He<sup>3</sup> elastic scattering is predominant. A complex pileup spectrum was observed at these angles exhibiting 12 spurious peaks of equal intensity which looked like groups of particles of energies between 25 and 50 MeV. The pileup pulses, when viewed on an oscilloscope, were observed to be due to a superposition of two 1-μsec-wide pulses of two separate elastic events, occurring

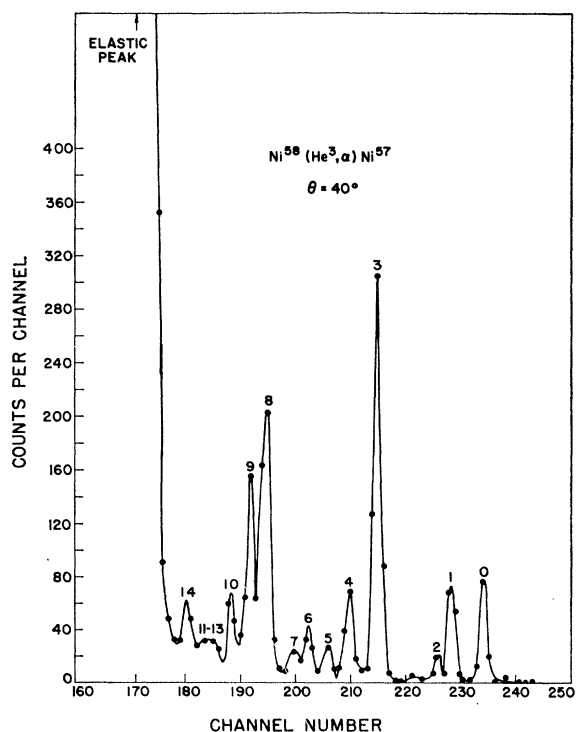


FIG. 1. (He<sup>3</sup>, α) spectrum from Ni<sup>58</sup> at the laboratory scattering angle of 40°.

<sup>12</sup> J. S. Allen, S. Chatterjee, L. E. Ernest, and A. I. Yavin, Rev. Sci. Instr. **31**, 831 (1960).

$n \times 0.08 \mu\text{sec}$  apart, where  $n = 1, 2, \dots, 12$ , and  $0.08 \mu\text{sec}$  ( $\approx \frac{1}{2} MH^{-1}$ ) is the time interval between two successive rf pulses from the cyclotron. This trouble was eliminated by decreasing the beam intensity until no peak twice the energy of the elastic scattering peak was observed. [This point is presented here in order to illuminate a difficulty which can be encountered in the use of rf-pulsed accelerators when low probability processes such as  $(\text{He}^3, \alpha)$  are investigated in the presence of a high probability process such as elastic scattering.]

III. EXPERIMENTAL RESULTS

Typical spectra for  $\text{Ni}^{58}(\text{He}^3, \alpha)\text{Ni}^{57}$  and  $\text{Ni}^{60}(\text{He}^3, \alpha)\text{Ni}^{59}$  are shown in Figs. 1 and 2, respectively. Data were taken between the laboratory scattering angles of  $15^\circ$  and  $90^\circ$  at intervals of  $5^\circ$ . The elastic-scattering peak in Fig. 1 contains approximately  $14 \times 10^4$  counts. The arrow indicates its location. To avoid using excessive machine time, a run was terminated when several hundred counts had accumulated in the most prominent of the  $(\text{He}^3, \alpha)$  peaks (peak 3 for  $\text{Ni}^{57}$  and peak 6 for  $\text{Ni}^{59}$ ). A few peaks could not be resolved at some angles. The excitation energies corresponding to these peaks were determined only from runs in which the peaks could be clearly resolved. Our experimental values for the excitation energies are tabulated in Table I. Aster-

TABLE I. Observed peak excitation energies and suggested spins and parities. (Asterisks denote peaks which appear to be single at all scattering angles within our experimental resolution.)

$\text{Ni}^{57}$			$\text{Ni}^{59}$		
Peak	Excitation energy (MeV)	Spin and parity	Peak	Excitation energy (MeV)	Spin and parity
0	0	$\frac{3}{2}^-$	0	0	$\frac{3}{2}^-$
1	.76*	$\frac{3}{2}^-$	1	.35	$\frac{3}{2}^-$
2	1.08*	$\frac{3}{2}^-$ or $\frac{3}{2}^+$	2	.87*	$\frac{3}{2}^-$
3	2.58*	$\frac{7}{2}^-$	3	1.33	$\frac{3}{2}^-$
4	3.26	$\frac{3}{2}^-$	4	1.70*	$\frac{3}{2}^-$
5	3.83	$\frac{3}{2}^-$	5	1.96*	$\frac{7}{2}^-$
6	4.26*	$\frac{3}{2}^-$	6	2.67*	$\frac{7}{2}^-$
7	4.59	$(\frac{3}{2}^-)$	7	3.10	$\frac{7}{2}^-$
	4.95 (weak)		8	3.73	
8	5.28*	$\frac{7}{2}^-$	9	4.25	
9	5.66		10	4.76	
10	6.12	$\frac{7}{2}^-$	11	5.31	
11	6.61		12	5.74	
12	6.80		13	6.60	
13	7.01		14	7.52	
14	7.18				

isks denote the peaks, which appear to be single at all scattering angles within the limits of our resolution. Our excitation energies are estimated to be accurate to within  $\pm 35 \text{ keV}$ . These results are in good agreement with other data.

Figure 3 presents the angular distributions associated with the ground state and the first ten excited states of  $\text{Ni}^{57}$ . The angular distributions are displaced vertically and a broken logarithmic ordinate scale is used. The

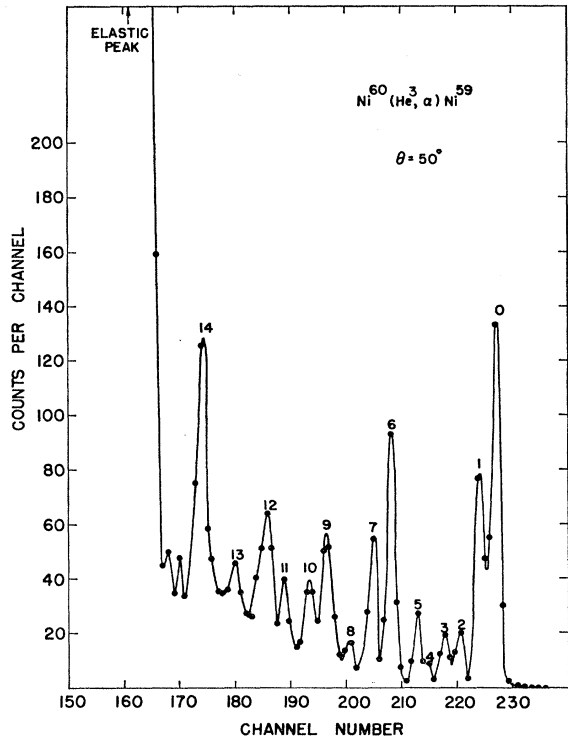


FIG. 2.  $(\text{He}^3, \alpha)$  spectrum from  $\text{Ni}^{60}$  at the laboratory scattering angle of  $50^\circ$ .

power of 10 near or just below the  $15^\circ$  point indicates the relative magnitude of that point. Smooth dashed curves are drawn through the experimental points. Error bars represent the statistical uncertainty. Figure 4 shows the relative angular distributions of the ground state and the next seven resolvable peaks in  $\text{Ni}^{59}$  in the same manner as in Fig. 3. Since many of the  $\text{Ni}^{59}$  peaks were weakly excited, the statistical uncertainties in some cases are large. Peak 1 is known to contain two levels of different  $l$  values,<sup>6,7,10</sup> but the  $l=1$  level, which could be resolved only at a few angles was always found to be very weak relative to the main  $l=3$  peak.

IV. DISCUSSION

Before we discuss the levels of  $\text{Ni}^{57}$  and  $\text{Ni}^{59}$  separately, it is well to review the information available on the states for which level assignments are quite well established from previous pickup and stripping work.<sup>3,6-11</sup> In particular,  $l=1$  angular momentum transfers have been established for the ground states of  $\text{Ni}^{57}$  and  $\text{Ni}^{59}$  and the 0.87 and 1.33-MeV states of  $\text{Ni}^{59}$ .  $l=3$  transitions have been established for the 0.76- and 2.58-MeV states of  $\text{Ni}^{57}$  and the 0.35- and 2.67-MeV states of  $\text{Ni}^{59}$ . Moreover, the spins and parities of these levels have also been established:  $j^\pi = \frac{3}{2}^-$  for the ground states of  $\text{Ni}^{57}$  and  $\text{Ni}^{59}$  and the 0.87-MeV state of  $\text{Ni}^{59}$ ;  $j^\pi = \frac{1}{2}^-$  for the 1.33-MeV state of  $\text{Ni}^{59}$ . In addition  $j^\pi = \frac{5}{2}^-$  for the 0.76-MeV state of  $\text{Ni}^{57}$  and the 0.35-MeV state of

Ni<sup>59</sup>, whereas  $j^\pi = \frac{3}{2}^-$  for the 2.58-MeV state of Ni<sup>57</sup> and the 2.67-MeV state of Ni<sup>59</sup>.

We accept these assignments as valid in drawing conclusions for some of the other states observed in our

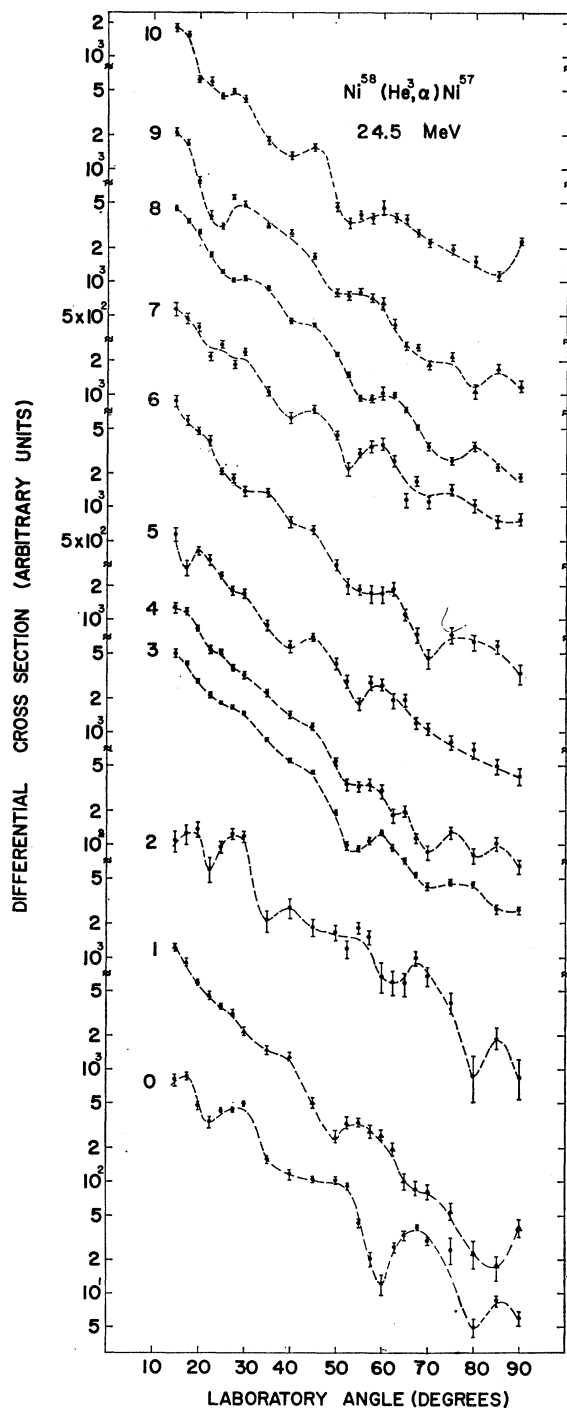


FIG. 3. Angular distributions of alphas from Ni<sup>58</sup>. The distributions are displaced vertically. The power of 10 near or just below the 15° point indicates the relative magnitude of that point.

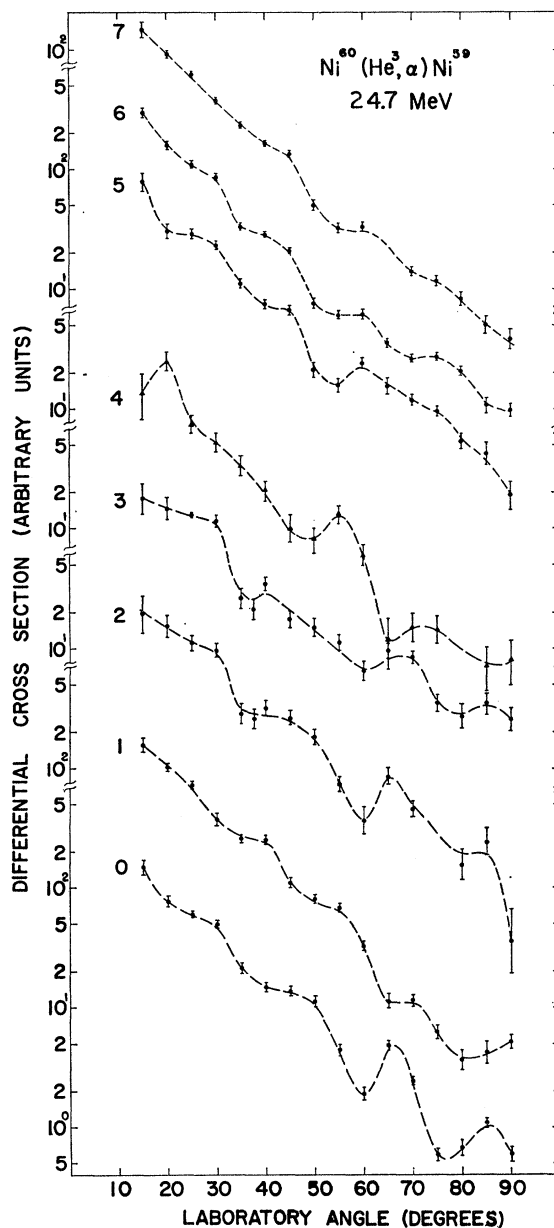


FIG. 4. Angular distributions of alphas from Ni<sup>60</sup>. The distributions are displaced vertically. The power of 10 near or just below the 15° point indicates the relative magnitude of that point.

data. We first constructed a "standard" angular distribution, based on the accepted  $j^\pi = \frac{3}{2}^-$  states listed above and shown in Fig. 5. These states are labelled Ni<sup>57</sup> 0, Ni<sup>59</sup> 0, and Ni<sup>59</sup> 2, the numbers 0 and 2 referring to the ordering shown in Table I. The three distributions are practically identical. This suggests that the distributions depend primarily on  $l$  and  $j$ , but not sensitively on the  $Q$  value. The dashed curve in this figure is one passed through the data points of the 1.33-MeV state in Ni<sup>59</sup> which we take to represent a  $j^\pi = \frac{1}{2}^-$  angu-

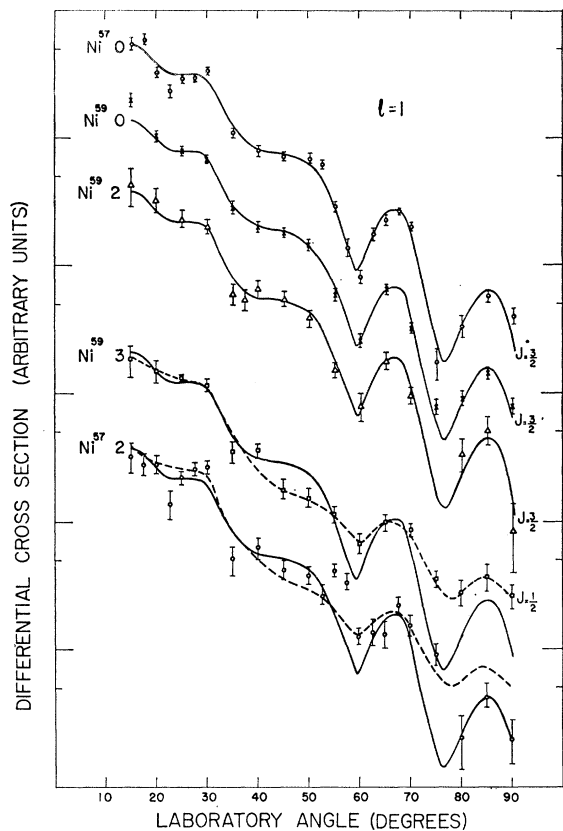


FIG. 5.  $l=1$  angular distributions. The top three distributions correspond to the known  $j^\pi = \frac{3}{2}^-$  states in  $\text{Ni}^{57}$  and  $\text{Ni}^{59}$ . The next distribution corresponds to the known  $j^\pi = \frac{3}{2}^-$  state in  $\text{Ni}^{59}$ . The solid curve in each distribution is the standard  $j^\pi = \frac{3}{2}^-$  curve derived from the known  $j^\pi = \frac{3}{2}^-$  distributions. The dashed curves represent the  $j^\pi = \frac{1}{2}^-$  distribution. The numbers adjacent to the distribution correspond to the peaks of Table I.

lar distribution. Similarly, in Fig. 6 the solid curve represents our data for the accepted  $\frac{7}{2}^-$  states at 2.58 MeV in  $\text{Ni}^{57}$  and at 2.67 MeV in  $\text{Ni}^{59}$ , and the dashed curve represents our data for the accepted  $\frac{5}{2}^-$  states at 0.76 MeV in  $\text{Ni}^{57}$  and at 0.35 MeV in  $\text{Ni}^{59}$ . Angular distributions for several other known  $l=1$  and  $l=3$  transitions are also, respectively, displayed in Figs. 5 and 6.

It is clear that all the angular distributions of Fig. 5 resemble one another insofar as locations of peaks and valleys are concerned, but differ from the angular distributions of Fig. 6. Moreover, it is apparent from these data that a  $j$  dependence of the angular distributions exists as has been found previously in  $(d,p)$ ,<sup>11</sup>  $(p,d)$ ,<sup>7,9</sup>  $(d,t)$ ,<sup>13</sup> and  $(\alpha,p)$ <sup>14</sup> reactions. A possible  $j$  dependence for the  $l=1$  angular momentum transfer is suggested by the fact that the oscillations of the angular distributions for

$j = \frac{1}{2}$  are less pronounced in our angular interval than they are for  $j = \frac{3}{2}$ . Also, the angular distributions for the  $\frac{3}{2}^-$  states fall off more sharply between  $70^\circ$  and  $90^\circ$  than for the  $\frac{1}{2}^-$  state. On the basis of this behavior it could be suggested, for example, that the  $l=1$  state at 1.08 MeV in  $\text{Ni}^{57}$  is a  $\frac{3}{2}^-$  state. (See the curve labelled  $\text{Ni}^{57} 2$  in Fig. 5.) It is well to emphasize here that such an assignment depends upon the assignment of the 1.33 MeV state of  $\text{Ni}^{59}$  as having  $j^\pi = \frac{1}{2}^-$ . This is

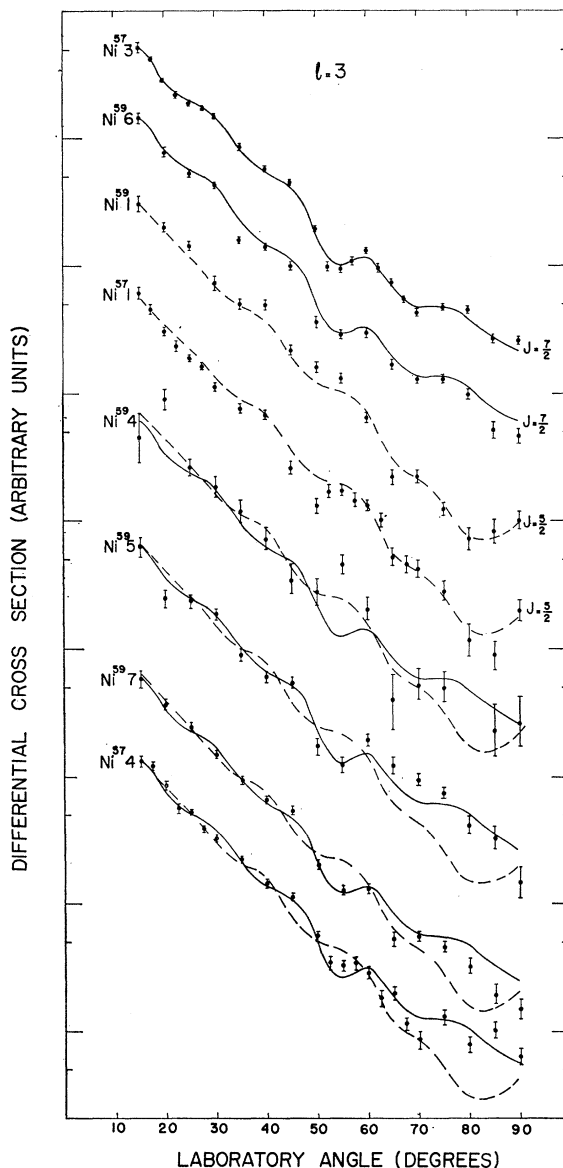


FIG. 6.  $l=3$  angular distributions. The top two distributions correspond to the known  $j^\pi = \frac{7}{2}^-$  states in  $\text{Ni}^{57}$  and  $\text{Ni}^{59}$ . The next two distributions correspond to the known  $j^\pi = \frac{5}{2}^-$  states in  $\text{Ni}^{57}$  and  $\text{Ni}^{59}$ . The solid curve in each distribution is the standard  $j^\pi = \frac{7}{2}^-$  curve extracted from the two known  $j^\pi = \frac{7}{2}^-$  distributions. The dashed curve in each distribution is the standard  $j^\pi = \frac{5}{2}^-$  curve extracted from the two known  $j^\pi = \frac{5}{2}^-$  distributions. The numbers adjacent to the distributions correspond to the peaks of Table I.

<sup>13</sup> R. H. Fulmer and W. W. Daehnick, Phys. Rev. Letters **12**, 455 (1965).

<sup>14</sup> L. L. Lee, Jr., A. Marinov, C. Mayer-Böricke, J. P. Schiffer, R. H. Bassel, R. M. Drisko, and G. R. Satchler, Phys. Rev. Letters **14**, 261 (1965).

consistent with most previously reported assignments<sup>8,9,11,15,16</sup> but disagrees with the work of Bartholomew and Gunye.<sup>17</sup> Figure 6, which presents the angular distributions for  $l=3$ , also shows a  $j$  dependence. The angular distributions of the two known  $\frac{5}{2}^-$  states appear to be different at around  $55^\circ$  than those of the two known  $\frac{7}{2}^-$  states. In addition, the  $\frac{5}{2}^-$  states seem to have a pronounced dip at about  $80^\circ$  and are rising at  $90^\circ$ , whereas the angular distribution of the  $\frac{7}{2}^-$  states appear to fall off more smoothly in this region. This behavior, if characteristic, suggests that the  $l=3$  states at 3.26 MeV in Ni<sup>57</sup> and at 1.96 and 3.10 MeV in Ni<sup>59</sup> are  $\frac{7}{2}^-$  states. There are other states such as the 1.70-MeV state in Ni<sup>59</sup> which seem to indicate  $l=3$  characteristics, but it is difficult to suggest any spin and parity for them on the basis of these criteria.

In order to accentuate the similarities and differences among the angular distributions of the same  $l$  value, we analyzed our data by a second method similar to the one used by Fulmer and Daehnick in their analysis of  $(d,t)$  angular distributions.<sup>13</sup> In Fig. 7 we show the ratio of the cross section leading to the 2.58-MeV state ( $j^\pi = \frac{7}{2}^-$ ) to the cross section leading to the 0.76-MeV state ( $j^\pi = \frac{5}{2}^-$ ) in Ni<sup>57</sup> (top curve), and the ratio of the cross section leading to the 2.67-MeV state ( $j^\pi = \frac{7}{2}^-$ ) to the cross section leading to the 0.35-MeV state ( $j^\pi = \frac{5}{2}^-$ ) in Ni<sup>59</sup> (middle curve). The dashed curves smoothly connect the points. There is a striking similarity between

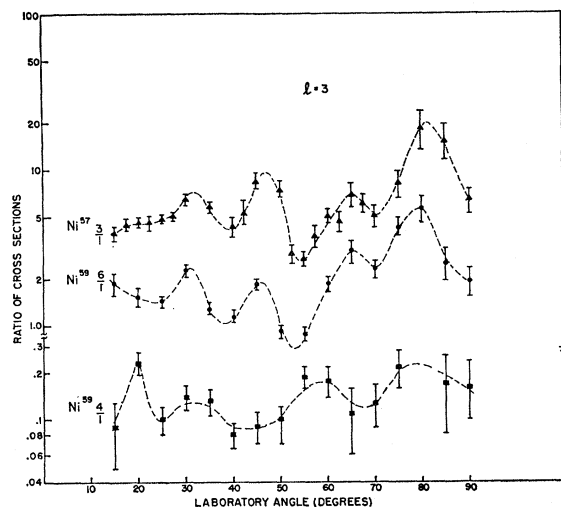


FIG. 7. Ratio of cross sections for  $l=3$ . The top curve is the ratio for the prominent  $\frac{7}{2}^-$  state (state 3, at 2.58 MeV) to the known  $\frac{5}{2}^-$  state (state 1, at 0.76 MeV) in Ni<sup>57</sup>. The middle curve is the ratio for the prominent  $\frac{7}{2}^-$  state (state 6, at 2.67 MeV) to the known  $\frac{5}{2}^-$  state (state 1, at 0.35 MeV) in Ni<sup>59</sup>. The bottom curve is the ratio for the state at 1.70 MeV to the  $\frac{5}{2}^-$  state at 0.35 MeV in Ni<sup>59</sup>. The dashed curves smoothly connect the points.

<sup>15</sup> B. L. Cohen, R. H. Fulmer, and A. L. McCarthy, Phys. Rev. **126**, 698 (1962).

<sup>16</sup> R. E. Coté, H. E. Jackson, Jr., L. L. Lee, Jr., and J. P. Schiffer, Phys. Rev. **135**, B52 (1962).

<sup>17</sup> G. A. Bartholomew and M. R. Gunye, Bull. Am. Phys. Soc. **8**, 367 (1963).

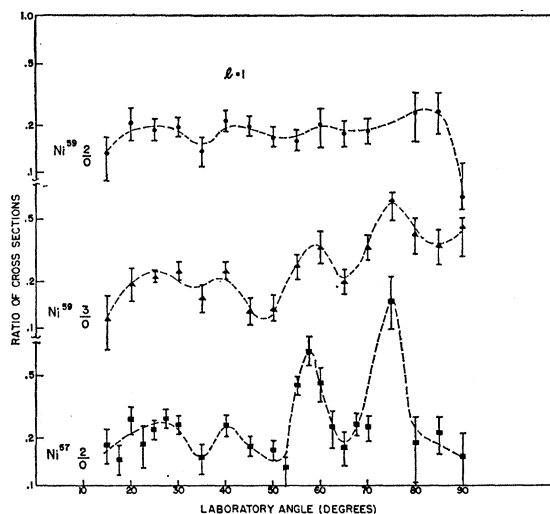


FIG. 8. Ratio of cross sections for  $l=1$ . The top curve is the ratio for the  $\frac{3}{2}^-$  state (state 2, at 0.87 MeV) to the  $\frac{3}{2}^-$  ground state, and the middle curve is the ratio for the  $\frac{1}{2}^-$  state (state 3, at 1.33 MeV) to the  $\frac{3}{2}^-$  ground state, both curves for Ni<sup>59</sup>. The bottom curve is the ratio for the state at 1.08 MeV to the  $\frac{3}{2}^-$  ground state in Ni<sup>57</sup>. The dashed curves smoothly connect the points.

these two oscillatory curves, both having four distinct peaks at the approximate angles of  $32^\circ$ ,  $46^\circ$ ,  $65^\circ$ , and  $81^\circ$ . A similar oscillatory behavior has recently been reported for iron.<sup>4</sup> We accept this behavior of the  $(\frac{7}{2}^-)/(\frac{5}{2}^-)$  cross sections as characteristic and use it to analyze states 4 through 10 of Ni<sup>57</sup> and states 4, 5, and 7 of Ni<sup>59</sup> (Table I). The following assignments follow:  $j^\pi = \frac{7}{2}^-$  for the states at 3.26, 3.83, 4.26, 5.28, 6.12, and possibly 4.59 MeV in Ni<sup>57</sup>, and for the states at 1.96 and 3.10 MeV in Ni<sup>59</sup>. On the other hand, the weakly excited state at 1.70 MeV in Ni<sup>59</sup>, which corresponds to  $l=3$ ,<sup>10</sup> has a distinctly different behavior. In fact, the ratio of the cross section leading to this state to the cross section leading to the  $\frac{5}{2}^-$  state at 0.35 MeV is almost constant (see Fig. 7, bottom curve), suggesting that this state has  $j^\pi = \frac{5}{2}^-$ . It should be noted here that these assignments presuppose  $l=3$  for all these states, whereas only the states at 3.26, 4.26, and 5.28 MeV in Ni<sup>57</sup> and at 1.70 and 1.96 MeV in Ni<sup>59</sup> have been consistently assigned  $l=3$  in the literature. Our spin assignments for the states at 3.26, 4.26, and 5.28 MeV in Ni<sup>57</sup> and at 1.96 and 3.10 MeV in Ni<sup>59</sup> agree with assignments in recent  $(p,d)$  work.<sup>9</sup>

In Fig. 8 we show (top curve) the ratio of the cross section leading to the 0.87-MeV state ( $j^\pi = \frac{3}{2}^-$ ) to the cross section leading to the ground state ( $j^\pi = \frac{3}{2}^-$ ), and (bottom curve) the ratio of the cross section leading to the 1.33-MeV state ( $j^\pi = \frac{1}{2}^-$ ) to the cross section leading to the ground state, both in Ni<sup>59</sup>. The dashed curves smoothly connect the points. The  $(\frac{3}{2}^-)/(\frac{3}{2}^-)$  ratio is clearly constant, whereas the  $(\frac{1}{2}^-)/(\frac{3}{2}^-)$  ratio peaks at approximately  $58^\circ$  and  $75^\circ$ . If this behavior is characteristic, the state at 1.08 MeV in Ni<sup>57</sup>, whose ratio of cross

section to the  $\frac{3}{2}^-$  ground-state cross section strongly peaks at approximately  $58^\circ$  and  $75^\circ$  (see bottom curve of Fig. 8), should be assigned  $j^\pi = \frac{1}{2}^-$ . Such an assignment contradicts the assignment suggested earlier in the paper and we conclude that on the basis of this experiment we are unable to assign a definite spin to this state.

### V. SUMMARY

To summarize this report, we have, by using the  $(\text{He}^3, \alpha)$  reaction been able to clearly identify a number of states in  $\text{Ni}^{57}$  and  $\text{Ni}^{59}$  which have not previously been reported in the literature. The fact that the  $(\text{He}^3, \alpha)$  reaction preferentially selects  $l=3$  states to  $l=1$  states has allowed us with an energy resolution of 120 keV to observe the 0.35-MeV state of  $\text{Ni}^{59}$  virtually unmasked by the 0.48-MeV state. We also have observed evidence for a  $j$  dependence in  $(\text{He}^3, \alpha)$  reactions, and have used

this evidence to suggest  $j$ -value assignments, as shown in columns 3 and 6 of Table I. Needless to say, we have based our conclusions concerning  $j$  dependence on a small number of cases. Much more detailed experimental work with a variety of targets and  $Q$  values is clearly needed, and we are continuing our program to that end. We are, at present, comparing our data to distorted-wave Born approximation predictions, and will report on this at a later time.

### ACKNOWLEDGMENTS

We are happy to acknowledge the helpful discussions we have had with Professor J. S. Allen, Professor P. Axel, and Professor M. E. Rickey. We are grateful to Professor R. Sherr for suggesting to us the usefulness of plotting ratios of cross sections. We also thank L. E. Ernest and the cyclotron staff for their cooperation in this experiment.

## Nuclear Recoil and Simple Nuclear Reactions\*

PAUL A. BENIOFF AND LUCY WU PERSON  
Argonne National Laboratory, Argonne, Illinois  
(Received 12 July 1965)

The nuclear-recoil properties of simple nuclear reactions are studied in the distorted-wave impulse approximation. Calculations of the differential recoil cross section  $d^2\sigma/d\Omega_K dT_K$ , and the recoil angular distribution  $d\sigma/d\Omega_K$ , for the  $\text{C}^{12}(p, pn)\text{C}^{11}$  and  $\text{Ni}^{58}(p, pn)\text{Ni}^{57}$  reactions at 450 MeV are presented and discussed. Relativistic kinematics are used and the calculations are not limited to coplanar events: they are valid for any type of kinematically allowed event. Harmonic-oscillator and exponential radial wave functions are used along with a complex, energy-dependent, Woods-Saxon optical potential. The calculations show appreciable differences between the exponential and harmonic-oscillator forms and also between distorted- and plane-wave calculations. In general, curves of  $d^2\sigma/d\Omega_K dT_K$  plotted as a function of  $T_K$  for fixed  $\theta_K$ , show steeper narrower peaks and larger flatter tails at  $\theta_K = 90^\circ$  than at  $\theta_K = 0^\circ$  or  $180^\circ$ . Comparison of the recoil angular distribution for outlying target neutron shells ( $1p$  in  $\text{C}^{12}$  and  $2p$  in  $\text{Ni}^{58}$ ) and interior shells ( $1s$  in  $\text{C}^{12}$  and  $1f$  in  $\text{Ni}^{58}$ ) shows a definite sideways peaking for the outlying shells which is lacking for the interior shells. This effect is explained as being a result of the equatorial localization of reaction sites which is greater for outer shells than for inner shells. Comparison with the small number of experimental data available indicates satisfactory agreement, except possibly for sideways recoil angles where, according to Rensberg, another reaction mechanism may be contributing.

### I. INTRODUCTION

IN recent years, the simple nuclear reactions have been under intensive investigation, mainly as  $(p, pn)$  and  $(p, 2p)$  reactions.<sup>1</sup> These studies have been concerned with such things as relative contributions from buried target shells,<sup>2-4</sup> characteristics of the target-nucleon wave function,<sup>4-7</sup> the structure of the target

nuclear state,<sup>8-10</sup> excitation functions,<sup>1,11</sup> etc. In many of these studies the momentum dependence of the square of the distorted-wave nuclear matrix element,

\* This work was performed under the auspices of the U. S. Atomic Energy Commission.

<sup>1</sup> J. R. Grover and A. A. Caretto, Jr., *Ann. Rev. Nucl. Sci.* **14**, 51 (1964). This review contains quite a complete bibliography of work done to date.

<sup>2</sup> H. Tyren, P. Hillman, and Th. A. J. Maris, *Nucl. Phys.* **7**, 1, 10 (1958).

<sup>3</sup> T. J. Gooding and H. Pugh, *Nucl. Phys.* **18**, 46 (1960).

<sup>4</sup> G. Tibell, O. Sundberg and P. U. Renberg, *Arkiv Fysik* **25**, 433 (1963).

<sup>5</sup> K. L. Lim and I. E. McCarthy, *Phys. Rev.* **133**, B1006 (1964).

<sup>6</sup> T. Berggren and G. Jacob, *Nucl. Phys.* **47**, 481 (1963); *Phys. Letters* **1**, 258 (1962).

<sup>7</sup> J. P. Garron, J. C. Jacmart, M. Riou, C. Ruhla, J. Teillac, and K. Strauch, *Nucl. Phys.* **37**, 126, (1962); C. Ruhla, M. Riou, R. A. Ricci, M. Ardit, H. Doubre, J. Jacmart, M. Liu, and L. Valentin, *Phys. Letters* **10**, 326 (1964).

<sup>8</sup> V. V. Balashov and A. N. Boyarkina, *Nucl. Phys.* **38**, 629 (1962).

<sup>9</sup> A. B. Clegg, K. J. Foley, G. L. Salmon, and R. E. Segel, *Proc. Phys. Soc. (London)* **78**, 681 (1961); K. J. Foley, G. L. Salmon, and A. B. Clegg, *Nucl. Phys.* **31**, 43 (1962); S. M. Austin, G. L. Salmon, A. B. Clegg, K. J. Foley, and D. Newton, *Proc. Phys. Soc. (London)* **80**, 383 (1962).

<sup>10</sup> H. G. Pugh, D. L. Hendric, M. Chabre, and E. Boschitz, *Phys. Rev. Letters* **14**, 434 (1965).

<sup>11</sup> P. L. Reeder and S. S. Markowitz, *Phys. Rev.* **133**, B639 (1964); I. Levenberg, V. Pokrovsky, Rhen De-Hou, L. Tarasova, and I. Yutlandov, *Nucl. Phys.* **51**, 673 (1964).